PERFORMANCE TESTS OF AN EVACUATED FLAT PLATE SOLAR COLLECTOR UNDER A VIRTUAL IMAGE SOLAR SIMULATOR.

Roger Moss,[a] Stan Shire[a], Paul Henshall[b], Philip Eames,[b], Farid Arya[c] and Trevor Hyde[c]
[a] School of Engineering, University of Warwick, Coventry, CV4 7AL, UK
[b] Centre for Renewable Energy Systems Technology, Loughborough University, UK
[c] School of the Built Environment, University of Ulster, UK
Corresponding author: Dr R.W.Moss, r.moss@warwick.ac.uk

ABSTRACT

An evacuated flat plate collector has been built and tested in a solar simulator. A vacuum of <0.1 Pa was used to eliminate heat losses through convection and gas conduction.

CFD and stress calculations for the hydro-formed panels determined the material thickness and through-hole sizes. The simulator used a reflecting tube to generate uniform illumination via multiple virtual images of four halogen floodlights. Tests with and without vacuum over a range of illumination powers demonstrate the efficiency benefits of vacuum insulation when providing heat at elevated temperatures or with weak insolation.

INTRODUCTION

Evacuating a flat-panel solar collector will reduce its heat loss coefficient [1]. Reducing the pressure below 3500 Pa can prevent convection currents forming [2], with the result that heat losses through the gas are purely due to conduction. A further pressure reduction to below 0.5 Pa results in the molecular mean free path exceeding the separation of absorber and glass, so that conduction is largely eliminated also [3].

The principle is already widely applied in evacuated tube collectors [4] and offers the potential to deliver fluid at high temperatures (150-200°C) without the severe loss of efficiency that would occur at these temperatures if gas were present. Concentrating systems that focus light onto the tube can achieve high overall efficiencies but rely upon direct sunlight and a tracking system; non-concentrating tubes generally have a poor spatial fill factor. Flat plate collectors have a high fill factor and offer the potential for working at high temperature even with diffuse illumination. A 0.5*0.5m solar collector has been built and tested under a solar simulator.

NOMENCLATURE

G	[W/m^2]	Irradiance from solar simulator
T	[K]	Temperature
T_m^*	[m^{2}K/W]	Scaled temperature difference
W	[W]	Electrical power input to floodlights
C	[J/kgK]	Coolant specific heat capacity
$\dot{m}$	[kg/s]	Coolant mass flow rate
w	[m]	Absorber width, 0.47 m
α		Coating absorptance
η		Collector efficiency
τ		Glass transmittance

Subscripts

a	Ambient, air
i	Flow inlet to absorber
o	Flow outlet from absorber
m	Absorber mean

ENCLOSURE

Two styles of enclosure are being studied as part of this programme: one with glass front and back [5] and one with a glass front attached to a metal tray [6,7]. The data presented here is from the metal tray design: the double glass results will be reported in a later paper.

The glass is 6 mm thick Pilkington Optiwhite. The tray was fabricated from 0.5 mm thick 400 series stainless steel; after inserting the absorber, the glass was soldered to the tray using Cerasolzer [6]. The support pins that resist atmospheric pressure and hold the glass and tray apart were 7 mm diameter and 20 mm long.

The use of a relatively thin steel tray is advantageous as its flexibility leads to uniform loading over the support pins without needing the steel to be accurately flat before suck-down.

The four corners of the absorber were located in slotted brackets at each corner of the tray. These supported the weight of the absorber whilst allowing some thermal expansion and possible slight distortion due to the internal-to-external pressure difference across the absorber. Given the relatively poor thermal conductivity of stainless steel, point contact against these brackets was deemed acceptable without the need for additional insulating spacers to reduce heat conduction from absorber to tray.

Figure 1. Absorber plates after hydro-forming and laser cutting. The large hole in the baseplate transfers fluid between the two halves of the absorber.

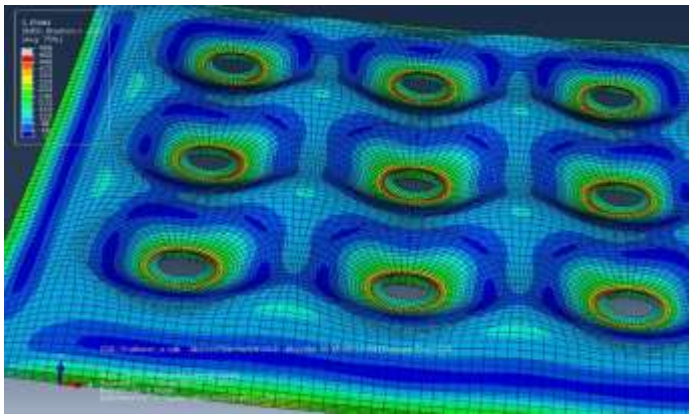

Figure 3. An Abaqus simulation of stresses resulting from internal pressures; in this model both sheets were 0.8 mm thick. Deflections are exaggerated for clarity.

ABSORBER DESIGN

Previous studies [8] have shown that the optimum dimension of channels for a micro-channel design or plate spacing for a flooded design is in the range 1.5-3 mm depending on the power used for pumping the coolant. These dimensions can reliably be achieved by hydroforming and welding thin plates together.

The collector consists of a pair of 0.7 mm thick hydro-formed plates TIG-welded onto a 0.9 mm baseplate; all are 316 stainless steel. Following previous design experience for micro-channel plate manifolds [8], it was concluded that better flow uniformity would be achieved if the square profile of the absorber were built as a pair of rectangles, with the flow mostly running lengthwise in each. The flow enters and leaves each rectangle at opposite corners (a "Z" configuration in micro-channel terms).

This allowed a simpler hydro-forming apparatus and, with a semi-single sided design, the welding of the left-hand hydro-formed plate "on top" and the right-hand one "underneath" minimised distortion without the need for pressing and welding a pair of symmetrical plates. A 28 mm diameter hole though the base plate transfers the fluid from the top left half to the underneath right half, Figure 1.

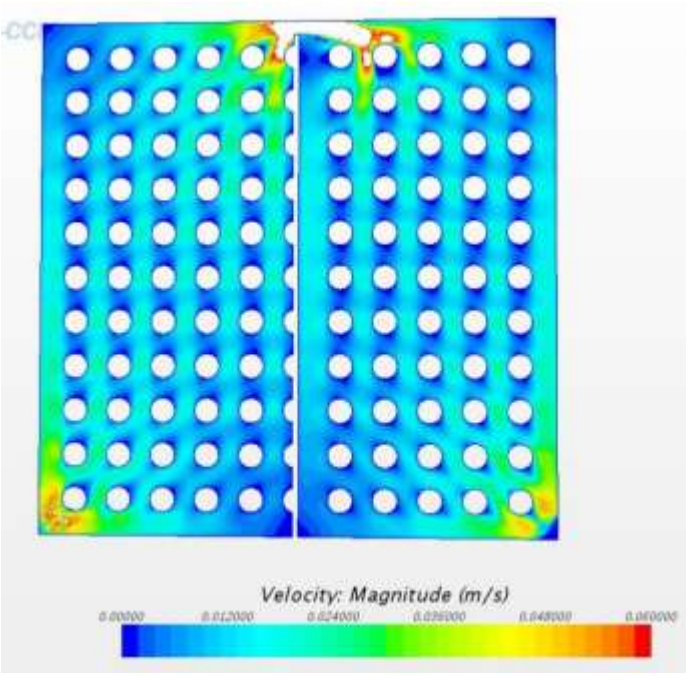

Figure 2. Star-CCM simulation of water flow within the collector.

Figure 4. Hydroforming apparatus. The clamp plates are 623×411×87 mm and weigh approximately 170 kg. A crane with a magnetic chuck is needed when separating the parts.

The flow distribution was modelled in Star-CCM (Figure 2) and found to be acceptable as regards providing cooling over the whole surface. A second consideration, that the pressure drop should be as low as practicable, was addressed by locally dishing the plates in the inlet and outlet regions to increase the plate spacing from 2 to 4 mm.

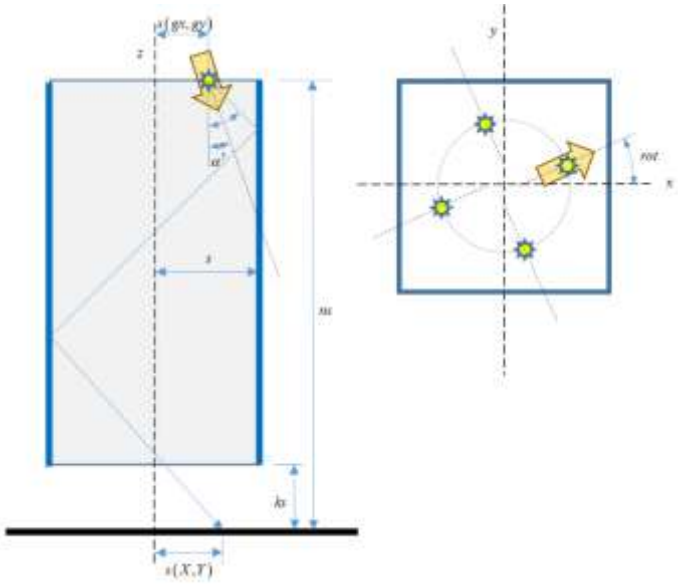

Figure 5. Virtual image simulation parameters.

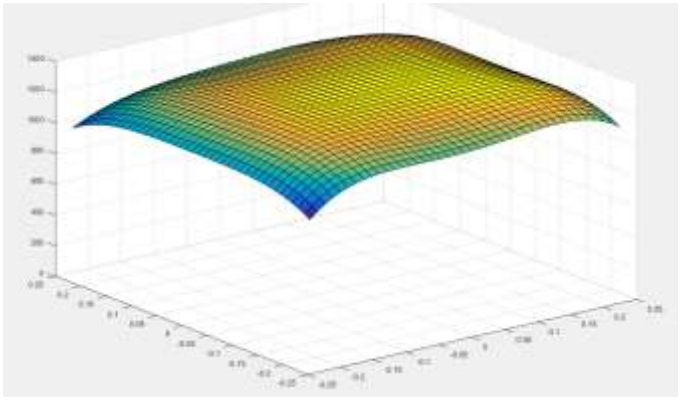

Figure 7. Measured illumination over absorber area, 5×5 grid fitted with polynomial surface (4 floodlights).

The material thickness, 0.7 mm, is a compromise between operational stresses in the vacuum enclosure (>1 bar pressure differential) and ease of hydroforming.

Finite Element modelling of the stresses in Abaqus (Figure 3) showed that the weld around each through-hole was the most highly stressed region: stresses were reduced by making the weld ring diameter (20mm) larger than the through hole (13 mm), Figure 3.

ABSORBER FABRICATION

The hydroforming facility, Figure 4, used a pair of thick clamping plates and a thin die plate, all machined from S355 steel. An O-ring sealed the stainless sheet against the lower clamp plate. Hydraulic oil at 25 MPa pushes the sheet onto the die to form both the overall depth and the support pin dimples, with M30 bolts holding the die plate firmly against the sheet to be formed. Each plate was then laser cut (Figure 1) and TIG welded to the base plate. Continuous-wave laser welding would

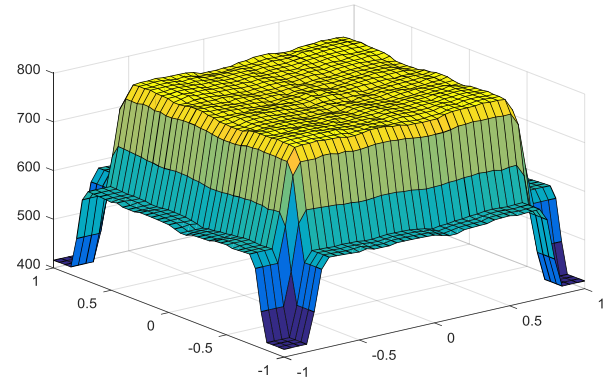

Figure 6. Matlab simulation of illumination levels (with 4 floodlights).

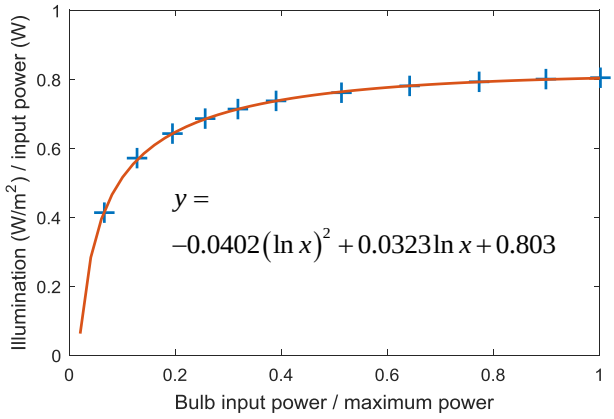

Figure 8. Illumination level at centre of absorber as a function of input power.

have been much quicker but the cost of developing the control program could not be justified given the small number of panels.

The welding causes some distortion. Measurements of the internal volume suggest the spacing between plates has reduced from the nominal 2 mm to approximately 1.6 mm.

The absorber was black chrome plated. Black chrome is a traditional selective absorber that can have good absorptivity at solar wavelengths and very low emissivity at long infra-red wavelengths, thereby minimising heat losses due to radiation.

The coating emissivity was measured using a Devices & Services AE1 emissometer and was approximately 0.46 over the centre but higher towards the edges.

SIMULATOR DESIGN AND COMMISSIONING

Performance testing of solar thermal collectors requires an illumination field sufficiently uniform that the mean illumination can be accurately determined from a number of point measurements. One approach is to use a large number of bulbs, covering an area considerably larger than the absorber; another, more efficient approach is to use reflective surfaces to provide virtual images of a smaller bulb area, thereby simulating a much

Figure 9. Solar simulator during commissioning tests, showing hinge and balance weights. The header tank and Variac are visible on the right-hand side; the vacuum system is on the left. Tank and pipe insulation were added later.

larger bulb field. Aluminium foil, bonded to the interior of a plywood box using "Spray Mount" adhesive, provides a simple but effective reflecting surface.

The illumination from a halogen floodlight was characterised over a 2D field by a series of pyranometer measurements. The variation in illumination with angle (altitude and azimuth) was used in a Matlab model to predict the illumination produced when multiple virtual images are added to the direct, line of sight illumination (Figure 6). The model predicted that a uniform illumination could be achieved over a large part of the box cross-section area.

The illumination was measured over a 5×5 grid matching the absorber dimensions. A polynomial surface fitted through these points (Figure 7) demonstrates the uniformity achieved. The area-average illumination was found by integration.

The four floodlights were powered by a Variac transformer and a Hameg HM8115-2 power meter measured the electrical power. A Kipp&Zonen CMP11 pyranometer was used to calibrate the illumination obtained over the 470 × 470 mm absorber area at full power and to determine the efficiency of the bulbs at reducer power levels, Figure 8. An empirical curve fitted these data points to within 0.7%. The simulator can

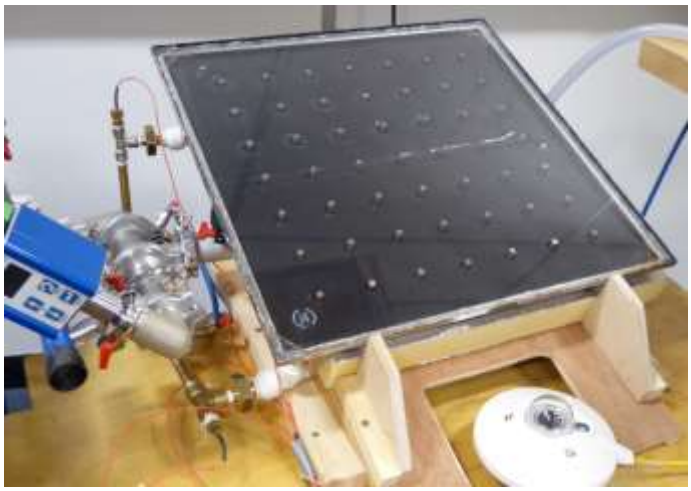

Figure 10. The collector prior to adding pipe insulation. Some of the inlet and outlet RTDs can be seen, together with the vacuum gauges and pyranometer. The collector tray sits on 50 mm thick Celotex insulation.

produce illumination levels up to 1300 W/m^2 but the highest used in these tests was 965 W/m^2.

The simulator was designed with a hinged box (Figure 9) that can be swung away from the collector for facilitate access. This requires some axial gap between end of the box and the illuminated surface and leads to illumination falling off towards the edges. To counter this effect the internal width of the box (700 mm) is larger than the solar collector (500 mm).

INSTRUMENTATION

A Huber Ministat 240 heater/chiller bath was used to pump water up to a header tank, from which a return loop allowed the water to circulate and kept the tank temperature close to the bath temperature. "Fernox" corrosion inhibitor was added to the water. The water was gravity-fed to the absorber and then passed via a Coriolis flow meter and needle valve back to the Huber bath.

Prior to testing the system was carefully filled with water to avoid any bubbles. Given the flooded panel nature of the absorber, with both inlet and outlet pipes approaching from below, it was important to ensure that the absorber could not collect a layer of bubbles that might impede heat transfer and lead to the metal temperature being significantly higher than the water temperature. The absorber was inclined at 17° to the horizontal so that small amounts of air, if present, would collect along the higher side rather than forming a continuous layer. As a further precaution, a bubble trap was placed between header tank and absorber to collect any bubbles that might come down the pipe and to indicate that this had happened. None were seen during testing and IR photographs of the glass temperature showed no indication of a void within the absorber.

The flow inlet and outlet temperatures were each measured by a pair of Pt100 RTDs, mounted in pipe fittings immediately adjacent to the panel connections. Glass and tray temperatures were measured using type T thermocouples bonded to the

surfaces using epoxy glue. Data acquisition was via a Measurement Computing USB-1616HS and Labview.

TESTING

Theory predicts that the conduction losses through the gas in the enclosure should disappear once the pressure falls below 1 Pa, for a typical absorber-collector spacing of order 5 mm.

Figure 11 shows the change in absorber heat flux as the gas pressure reduces. There is no illumination and the negative heat flux represents the heat losses due to conduction and radiation. This was during the warm-up period with hot water circulating through the collector.

At t = 57 minutes the diffusion pump valve is opened and the pressure (which was steadily falling with the backing pump) suddenly falls. From t = 62 minutes the pressure is below 0.5 Pa and the heat losses stabilise at the radiative level.

After 90 minutes, the collector temperature had stabilised at 74°, the glass at 37.4 and the tray at 43.2. Heat losses were 179.9 W/m^{2}K giving a heat loss coefficient U_L = 3.65 W/m^{2}K. This loss coefficient is higher than expected for a vacuum insulated collector because the black chrome plating was too thick and has an emissivity much higher than the optimum. The glass and tray had much longer time constants than the absorber (Figure 12). The corresponding heat loss coefficient for this collector at atmospheric pressure was of order 7 W/m^{2}K.

The tray gradually asymptotes towards the absorber temperature; the shallow gradient here at time t = 21 minutes represents a net heat input to the 0.5 mm thick tray of 10 W/m^2. Given enough rear insulation and sufficient time to completely reach equilibrium, this heat loss would fall to zero and the collector efficiency would rise accordingly.

The glass temperature is also slowly rising, largely due to it absorbing some of the light. In this case, radiative heat transfer between glass and collector leads to a gradual rise in the heat flux to the collector. A considerable settling period was allowed for all the efficiency tests, depending on the previous history and resulting tray and glass temperatures. The efficiency values presented below will however always be a slight underestimate due to never completely reaching time-steady equilibrium. A more detailed analysis of all this data will be published as a journal paper, together with data from future collectors.

Efficiency has been calculated in terms of the heat flux to the coolant, the absorber area and the illumination:

$$\eta = \frac{\dot{m}c\left(T_o - T_i\right)}{Gw^2}$$

w is the width of the black chrome plated absorber (not the glass). To allow sensible comparison with non-vacuum panels, the area of the through-holes has not been subtracted from the total. This matches the efficiency definition used by [9].

Most tests were performed with a water inlet temperature in the range 70-80°C, giving $T_m - T_a \approx 52°\text{C}$; the illumination was varied to achieve different values for $T_m^* = \frac{T_M - T_a}{G}$. The efficiency results are compared in Figure 13 with published data for three flat panels [9]. These published loss coefficients have

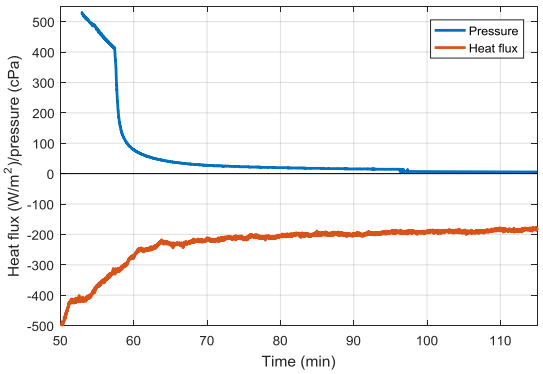

Figure 11. Hot water test with no illumination. As the pressure is reduced the heat losses decrease. Below 0.5 Pa the heat flux stabilises and is due to radiation only. Positive heat flux is defined as flowing *into* the panel: the negative values here indicate the heat loss rate.

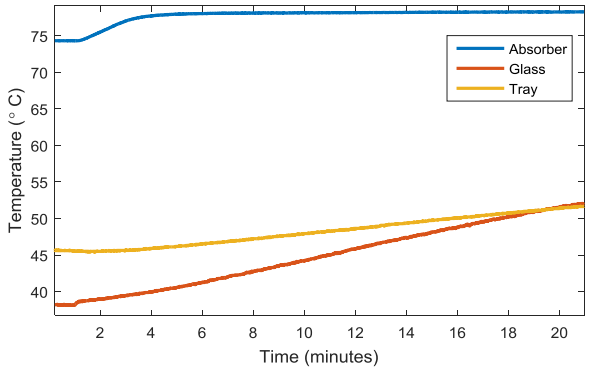

Figure 12. Transient test, G = 954 W/m^2, showing heat-up rates for absorber, glass and tray. $T_m = \left(T_i + T_o\right)/2$

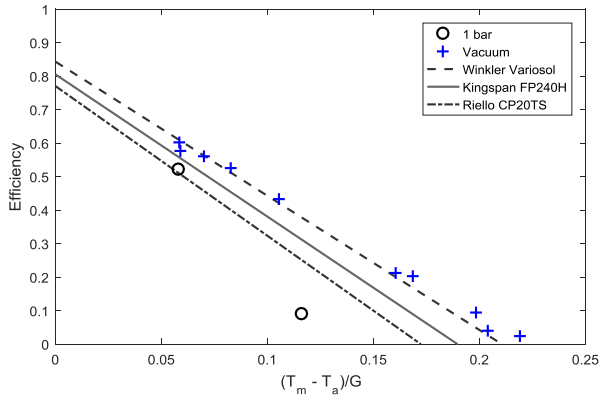

Figure 13. Measured collector efficiency, both at 1 bar and evacuated, compared with published data [9] for some conventional flat plate collectors made by Winkler, Kingspan and Riello. $T_m - T_a \approx 52°C$; G for the evacuated tests varies in the range 240 to 890 W/m^2.

been plotted for T_m^* and G values that correspond to the 52° temperature difference used in the current experiments. The lines are therefore straight as opposed to the conventional curves which result if $T_m - T_a$ is varied at constant G. If the heat loss from the collector is Q_L (constant since $T_m - T_a$ does not vary) and the heat absorbed is $G\tau\alpha$, the efficiency will be $\eta = \frac{G\tau\alpha - Q_L}{G} = \tau\alpha - \frac{Q_L}{G} = \tau\alpha - \frac{Q_L T_m^*}{52}$, hence the straight line.

The evacuated data is consistent with heat balance models using a mean coating absorptance of 0.9 and mean emissivity of 0.52. State of the art selective coatings [10] typically achieve absorptance = 0.95 and emissivity = 0.04. The black chrome plating used on the current collector has a much higher emissivity than this, leading to higher heat losses and lower efficiency than the best that might be possible with a high quality selective surface.

The experimental collector however, even with this very poor selective coating, achieves efficiencies comparable with one of the best-performers (the Riello CP20TS in Figure 13) from the SPF dataset. One can see, moreover, that there is a considerable difference in efficiency between the vacuum and non-vacuum results for the test collector. There is clearly the potential for a vacuum collector with a better coating to achieve much higher efficiencies.

In addition to the panel described here, a second panel with glass on both sides has been built and is being tested; a further five panels are under construction, including a simple reference case with a serpentine tube clamped to a 2 mm thick solid absorber plate. An earlier attempt at a serpentine tube construction, with the tube spot-welded to the plate, suffered leakage due to spot-weld failures (probably from thermal stresses) and could not be tested.

These future panels will have better selective coatings. They are expected to show considerable efficiency improvements over the collector described here.

CONCLUSION

A flat panel solar collector has been built and tested both under vacuum conditions and at atmospheric pressure. A significant increase in efficiency was achieved under evacuated conditions: despite having a very poor absorber coating, the efficiency when evacuated was comparable with some of the best (non-evacuated) commercial panels.

These results demonstrate the potential for high vacuum collectors at pressures less than 1 Pa to improve collector efficiency. Collector efficiency always falls as T_m^* increases due to the increase in heat losses relative to the illumination level: at any given delivery temperature the vacuum collector, since it eliminates gas conduction, has lower heat loss and higher efficiency than an equivalent non-evacuated panel.

This improvement in performance can extend the useful range of delivery temperatures relative to a conventional flat panel or, alternatively, provide useful efficiency levels at lower ambient temperatures or with lower irradiance than would commonly be feasible.

Evacuated flat panel collectors generally also offer significant advantages over the two alternatives for high delivery temperature. They typically have better spatial coverage than evacuated tube designs and, unlike concentrating systems, can operate without tracking and take advantage of diffuse illumination.

ACKNOWLEDGEMENTS

The authors are grateful to EPSRC for funding this work as part of a collaborative programme between Warwick, Loughborough and Ulster universities.

REFERENCES

[1] N. Benz and T. Beikircher, "High efficiency evacuated flat-plate solar collector for process steam production", *Solar Energy*. **65**, 1999, pp. 111-118.

[2] C. Eaton and H. Blum, "The use of moderate vacuum environments as a means of increasing the collection efficiencies and operating temperatures of flat-plate solar collectors", *Solar Energy*. **17**, 1975, pp 151-158.

[3] Shire, GSF, Moss, RW, Henshall, P, Arya, F, Eames PC and Hyde, T., Development of an Efficient Low- and Medium-Temperature Vacuum Flat-Plate Solar Thermal Collector, *Renewable Energy in the Service of Mankind Vol II;* 2016, p859-866, ISBN 9783319182148

[4] E. Zambolin and D. Del Col, "Experimental analysis of thermal performance of flat plate and evacuated tube solar collectors in stationary standard and daily conditions", *Solar Energy*. **84**, 2010, pp. 1382-1396.

[5] Arya, F., Hyde, T., Henshall, P., Eames, P., Moss, R. Shire, S., Zacharopoulos, A., Thermal Analysis of Flat Evacuated Glass Enclosure for Building Integrated Solar Applications, *Advanced Building Skins*, 2015, Bern, Switzerland.

[6] Henshall, P., Moss, R., Arya, F., Eames, P., Shire, S., Hyde, T., An Evacuated Enclosure Design for Solar Thermal Energy Applications. *Grand Renewable Energy Conference*, 2014, Tokyo, Japan.

[7] Henshall, P., Eames, P., Arya, F., Hyde, T.,Moss, R., Shire, S. (2016) Constant Temperature Induced Stresses in Evacuated Enclosures for High Performance Flat Plate Solar Thermal Collectors, *Solar Energy* April 2016 127:250-261

[8] Moss, R.W and Shire, G.S.F., "Design and performance of evacuated solar collector micro-channel plates", *EuroSun 2014 Conference Proceedings.*

[9] SPF Online Collector Catalogue, Institut Für Solartecknik website, www.spf.ch

[10] Almeco "Tinox Energy" brochure from the Almeco website, http://www.almecogroup.com/en/pagina/53-tinox-energy-cu